# COMPARISON BETWEEN MOLAR- AND MASS-BASED APPROACHES TO DROP EVAPORATION MODELLING

Tonini S.* and Cossali G.E.
*Author for correspondence
Department of Engineering and Applied Sciences,
Università di Bergamo,
Dalmine (BG), 24044
Italy
E-mail: simona.tonini @unibg.it

## ABSTRACT

Three evaporation models for single-component liquid drop floating in a gaseous environment are compared: two of them rely on the widely used assumption of constant (molar or mass) density and yield an explicit formula for the evaporation rate, while the third model relieves the constant density hypothesis yielding an implicit form of the evaporation rate. The comparison is made for a relative wide range of temperature and pressure operating conditions and for three liquids: water, n-octane and n-dodecane.

## INTRODUCTION

Modelling drop evaporation is of paramount importance in all those applied field where a correct estimation of vapour-gas mixture characteristics is necessary, like for example in a combustion environment. The main approach to the problem, based on some simplifying hypotheses like constancy of gas properties, spherical shape of the drop, quasi-steadiness, uniform drop temperature and composition and many others (see [1,2] for a thorough review) has led to a limited number of analytical models, among which [3] is the most widespread one, which are nowadays implemented in most of commercial and in-house CFD codes for dispersed flow modelling. Recently some of the above mentioned simplifications have been questioned [4,5] and a renewed interest for a more accurate modelling led to some improvements. The classical approach to model the vapour transport through the gas phases relies on the constancy of the gas density, which cannot obviously represents correctly the physics of the phenomenon when the gas and the drop temperatures differ noticeably. The above mentioned model that relieve such hypothesis [4], differently form the classical approach, yields the evaporation rate in implicit form, rendering computationally less efficient its implementation in CFD codes.

For single component drop evaporation, the widely accepted Stefan-Maxwell constitutive equations can be reduced to the well-known Fick's law, that can be expressed equivalently in molar or in mass form [6]. Simplified solution can then be obtained from both forms by imposing a different approximation (namely the constancy of the mass rather than the molar density) that yields different solutions.

The aim of the present work is to quantitatively investigate the role of each of the two approximations in order to evidence the effect on the quantitative prediction of the evaporation rate from a spherical drop floating in a gaseous environment.

## NOMENCLATURE

Roman symbols

| | | |
|---|---|---|
| $c_p$ | [J/kgK] | Specific heat at constant pressure |
| $c$ | [kmol/m$^3$] | Molar density |
| $D_{pk}$ | [m$^2$/s] | Binary diffusion coefficient |
| G | [-] | Logarithm of gas mass fraction |
| H | [-] | Logarithm of gas molar fraction |
| $\mathbf{J}$ | [kmol/m$^2$s] | Diffusive component of molar flux |
| $k$ | [W/mK] | Thermal conductivity |
| $Le$ | [-] | Modified Lewis number |
| $M$ | [-] | Mass/molar evaporation rate ratio |
| $m_{ev}$ | [kg/s] | Mass evaporation rate |
| $Mm$ | [kg/kmol] | Molar mass |
| $\mathbf{n}$ | [kg/m$^2$s] | Mass flux |
| $\mathbf{N}$ | [kmol/m$^2$s] | Molar flux |
| $N_{ev}$ | [kmol/s] | Molar evaporation rate |
| $P$ | [Pa] | Pressure |
| $r$ | [m] | Radial coordinate |
| $R$ | [J/kmolK] | Universal gas constant |
| $R_0$ | [m] | Drop radius |
| Re | [-] | Reynolds number |
| T | [K] | Temperature |
| $U$ | [m/s] | Stefan velocity |
| $y$ | [-] | Molar fraction |
| $Y$ | [-] | Non-dimensional evaporation rate |

Greek symbols

| | | |
|---|---|---|
| $\chi$ | [-] | Mass fraction |
| $\rho$ | [kg/m$^3$] | Mass density |
| $\Lambda$ | [-] | Non-dimensional number (equation 17) |
| $\theta$ | [-] | Molar mass ratio |
| $\zeta$ | [-] | Non-dimensional radial coordinate, $\zeta=R_0/r$ |

Subscripts

| | |
|---|---|
| $b$ | Boiling |
| $r$ | Radial component |
| $ref$ | Reference condition |
| $s$ | Surface |
| $T$ | Total |
| $v$ | Vapour |
| $\infty$ | Free stream condition |
| 0 | Ambient or reference |

| Superscripts | |
|---|---|
| mass | Mass |
| mol | Molar |
| (0) | Gas |
| (1) | Vapour |
| ~ | Non-dimensional |

## MATHEMATICAL MODELLING

The Stefan-Maxwell equations are considered the correct constitutive equations to model the diffusion of multicomponent species in a mixture, and a simple form for a mixture of n+1 species, neglecting Soret effect and diffusion due to pressure gradients and to external force, is [6]:

$$\nabla y^{(p)} = \sum_{k=0}^{n} \frac{1}{cD_{pk}} \left( y^{(p)} \mathbf{J}^{(k)} - y^{(k)} \mathbf{J}^{(p)} \right) \tag{1}$$

where $y^{(p)}$ is the molar fraction of the p-component, $\boldsymbol{J}^{(p)}$ is the diffusive molar flux of the p-component, $c$ is the molar density and $D_{pk}=D_{kp}$ are the binary diffusion coefficient of p-component into k-component. Since the total flux of a species is given by:

$$\mathbf{N}^{(p)} = y^{(p)} \mathbf{N}^{(T)} + \mathbf{J}^{(p)} \tag{2}$$

where $\mathbf{N}^{(T)} = \sum_{k=0}^{n} \mathbf{N}^{(k)}$ and $\mathbf{N}^{(T)} y^{(p)}$ is the convective component of the molar flux, the LHS of equation (1) can be transformed into the more useful form:

$$\nabla y^{(p)} = \sum_{k=0}^{n} \frac{1}{cD_{pk}} \left( y^{(p)} \mathbf{N}^{(k)} - y^{(k)} \mathbf{N}^{(p)} \right) \tag{3}$$

The evaporation of a multi-component drop can then be modelled on the basis of equation (3) and an exact solution for multi-component spherical drops can be found in [7].

Hereinafter the index 0 will always refers to the species that is not part of the liquid drop composition, some time referred also as "gas". When the evaporation of a single component drop is considered, the above constitutive equations can be simplified obtaining

$$\begin{aligned} \mathbf{N}^{(0)} &= y^{(0)} \mathbf{N}^{(T)} - cD_{10} \nabla y^{(0)} \\ \mathbf{N}^{(1)} &= y^{(1)} \mathbf{N}^{(T)} - cD_{10} \nabla y^{(1)} \end{aligned} \tag{4}$$

which is a way to state the Fick's law of diffusion [6]. To notice that the two equations are linearly dependent.

Considering now the species mass fluxes, that are related to the molar fluxes by $\mathbf{n}^{(p)} = \mathbf{N}^{(p)} Mm^{(p)}$, where $Mm^{(p)}$ is the $p$-component molar mass, equations (4) can be transformed into the most used mass form:

$$\begin{aligned} \mathbf{n}^{(0)} &= \chi^{(0)} \mathbf{n}^{(T)} - \rho D_{10} \nabla \chi^{(0)} \\ \mathbf{n}^{(1)} &= \chi^{(1)} \mathbf{n}^{(T)} - \rho D_{10} \nabla \chi^{(1)} \end{aligned} \tag{5}$$

where $\chi^{(p)}$ is the mass fraction of the $p$-species, which is related to the molar fraction by the rule:

$$y^{(p)} = \chi^{(p)} \frac{\rho Mm^{(p)}}{c} \tag{6}$$

The two forms are a direct consequence of S-M equations and they are equivalent only for the case of single component drop ($n$=1). When considering steady drop evaporation it is often assumed that the liquid-gas interface is still and the diffusion of the gas species through the liquid is neglectful, then it can be assumed that the gas flux is nil everywhere i.e. $\mathbf{n}^{(0)} = \mathbf{N}^{(0)} Mm^{(0)} = 0$. This assumption transforms equations (4) and (5) for the gas species into:

$$\mathbf{N}^{(T)} = cD_{10} \nabla \ln y^{(0)}; \quad \mathbf{n}^{(T)} = \rho D_{10} \nabla \ln \chi^{(0)} \tag{7}$$

The steady-state species conservation equations for both molar and mass cases are given by [6]:

$$\nabla \mathbf{N}^{(p)} = 0; \quad \nabla \mathbf{n}^{(p)} = 0 \tag{8}$$

and summation over the index $p$ yields the usual mass conservation equations:

$$\nabla \mathbf{N}^{(T)} = 0 \tag{9a}$$

$$\nabla \mathbf{n}^{(T)} = 0 \tag{9b}$$

Simple analytical solutions of (9a) and (9b) can be found imposing the constancy of the molar ($c$) or the mass ($\rho$) densities respectively. These assumptions are not equivalent and then the two equations, that are perfectly equivalent, yield instead different solutions. After imposing the constancy of either the mass or the molar density, using equation (7) and setting $H = \ln y^{(0)}$ and $G = \ln \chi^{(0)}$ equations (9a) and (9b) yield:

$$\nabla^2 H = 0 \tag{10a}$$

$$\nabla^2 G = 0 \tag{10b}$$

## CONSTANT DENSITY DROP EVAPORATION MODELS

The classical drop evaporation models are obtained by integrating equation (10b) in spherical coordinates with the B.C.:

$$G(R_0) = \ln \chi_s^{(0)} = G_s; \quad G(\infty) = \ln \chi_\infty^{(0)} = G_\infty \tag{11}$$

yielding:

$$G(r) = (G_s - G_\infty) \frac{R_0}{r} + G_\infty \tag{12}$$

and then evaluating the mass evaporation rate by:

$$m_{ev}^{mas} = 4\pi R_0^2 n_r^{(T)} = 4\pi R_0 \rho_{ref} D_{10} \ln \frac{1-\chi_\infty^{(1)}}{1-\chi_s^{(1)}} \tag{13}$$

(see for example [8]), where the value of the constant mass density $\rho_{ref}$ is usually evaluated at a reference condition through the "1/3-law" proposed by [9]. This equation, that holds for drop evaporation at Re=0 is the basis of the above mentioned

widespread model of Abramzon and Sirignano [3] that holds for large Re.

Similarly, equation (10a) can be integrated with the B.C.:

$$H(R_0) = \ln y_s^{(0)} = H_s; \quad H(\infty) = \ln y_\infty^{(0)} = H_\infty \tag{14}$$

yielding:

$$N_{ev} Mm^{(1)} = m_{ev}^{mol} = 4\pi R_0 c_{ref} D_{10} \ln \frac{1-y_\infty^{(1)}}{1-y_s^{(1)}} \tag{15}$$

where $c_{ref}$ can be evaluated again by the 1/3rd-rule. To notice that the mass evaporation rate $m_{ev}^{mas}$ is different from $m_{ev}^{mol}$, as above explained, since generally:

$$c_{ref} \ln \frac{1-y_\infty^{(1)}}{1-y_s^{(1)}} \neq \rho_{ref} \ln \frac{1-\chi_\infty^{(1)}}{1-\chi_s^{(1)}} \tag{16}$$

Since the second approach is as justified as the first one, it is worth to investigate which of them is the most accurate, if any. To this end the results of the two approaches can be compared with those obtained solving the conservation equations (9a,b) without assuming a constant molar or mass density.

## VARIABLE DENSITY DROP EVAPORATION MODEL

As above pointed out the molar and mass approach for single drop evaporation modelling yields different results only by the fact that the simplifying assumptions differ (constancy of molar either then mass density). A previous work [4] has shown that an analytical solution can be found by relieving the constant density assumption. The approach consists of assuming perfect gas behaviour for the gaseous phase and showing that for

$$\Lambda = \frac{RT_\infty R_0^2}{Mm^{(1)} D_{10,ref}} \to \infty \tag{17}$$

which is a quite acceptable assumption for practical applications, the momentum equation yields the constancy of the pressure across all the gas phase:

$$P_T = \left(1+\theta\chi^{(0)}\right)\rho \frac{RT}{Mm^{(1)}} = cRT = const. \tag{18}$$

where $\theta = \frac{Mm^{(1)} - Mm^{(0)}}{Mm^{(0)}}$. The gas temperature field can be found solving the energy equation in radial symmetry and neglecting minor terms like dissipation from viscous stresses, species excess kinetic energy, and work of pressure forces (see [6] for the complete equation):

$$\rho U c_p \nabla T - k\nabla^2 T = 0 \tag{19}$$

with first kind B.C.: $T(R_0) = T_s; \quad T(\infty) = T_\infty$, yielding:

$$\tilde{T} = \frac{1-\tilde{T}_s}{1-e^{-Y}} e^{-Y\zeta} + \frac{\tilde{T}_s - e^{-Y}}{1-e^{-Y}} \tag{20}$$

where: $\tilde{T} = \frac{T}{T_\infty}$, $\zeta = \frac{R_0}{r}$, $Y = \frac{m_{ev} c_{p,ref}}{4\pi R_0 k_{ref}}$ and $m_{ev}$ is the evaporation rate.

Allowing for the variability of the gas density the two forms (molar and mass) of the species conservation equation yield the same differential equation. The solution reported in [4] was derived from the mass form (9b) yielding the following implicit equation for the non-dimensional evaporation rate:

$$Y + \left(\tilde{T}_s - 1\right)\left(\frac{Y}{1-e^{-Y}} - 1\right) = \frac{1}{Le} \ln \left( \frac{\left(1+\theta\chi_\infty^{(0)}\right) - \frac{P_{v,s} Mm^{(1)}}{RT_\infty \rho_\infty}}{(1+\theta)\left(1-\chi_\infty^{(1)}\right)} \right) \tag{21}$$

where $Le = \frac{k_{ref}}{c_{ref} Mm^{(1)} D_{10,ref} c_{p,ref}}$ is the modified Lewis number evaluated at the reference temperature. It should be stressed that the numerical value of *Le* is very slightly dependent on the reference temperature since the temperature dependence of $k_{ref}$, $c_{ref}$ and $D_{10,ref}$ practically cancels out in *Le*. A simpler form can be obtained transforming equation (21) using the relations:

$$y^{(p)} = \frac{\rho}{cMm^{(p)}} \chi^{(p)}; \quad P_{v,s} = y_s^{(1)} P_T \tag{22}$$

or directly solving (9a) with the same method used in [4], yielding:

$$Y = \frac{c_\infty}{c_{ref} \int_0^1 \tilde{T} d\zeta} \frac{1}{Le} \ln \left( \frac{1-y_\infty^{(1)}}{1-y_s^{(1)}} \right) \tag{23}$$

where $\int_0^1 \tilde{T} d\zeta = \frac{\tilde{T}_s - e^{-Y}}{1-e^{-Y}} + \frac{1-\tilde{T}_s}{Y}$.

As reported in [5], the present and the above reported constant molar and mass density evaporation models can be extended to include the effect of convective flow through an approach based on the film theory (see also [3]).

## MODEL COMPARISON

The previous results about the evaporation rate can be written in non-dimensional form as:

$$Y^{mol} = \frac{m_{ev}^{mol} c_{p,ref}}{4\pi R_0 k_{ref}} = \frac{1}{Le} \ln \left( \frac{1-y_\infty^{(1)}}{1-y_s^{(1)}} \right) \tag{24a}$$

$$Y^{mass} = \frac{m_{ev}^{mas} c_{p,ref}}{4\pi R_0 k_{ref}} = \frac{\rho_{ref}}{c_{ref} Mm^{(1)}} \frac{1}{Le} \ln \left( \frac{1-\chi_\infty^{(1)}}{1-\chi_s^{(1)}} \right) \tag{24b}$$

$$Y = \frac{c_\infty}{c_{ref} \int_0^1 \tilde{T} d\zeta} \frac{1}{Le} \ln \left( \frac{1-y_\infty^{(1)}}{1-y_s^{(1)}} \right) \tag{24c}$$

where: $Y = \frac{m_{ev} c_{p,ref}}{4\pi R_0 k_{ref}}$ can be assumed to be a more accurate estimation of the non-dimensional evaporation rate since it has been obtained without imposing a constant gas density. Moreover the model has been validated in [5] against an extensive experimental data base, confirming a relatively good agreement between the model predictions and the measurements.

It should be noticed that the constant mass density model yields the same results as the constant molar density one only when $\theta$=0 (i.e. when $Mm^{(1)}= Mm^{(0)}$, like for example for a methanol drop evaporating in oxygen), in fact in such case:

$$\frac{\rho_{ref}}{c_{ref} Mm^{(1)}} = 1 \tag{25}$$

Moreover, for the isothermal case ($T_s$=$T_\infty$):

$$\frac{c_\infty}{c_{ref} \int_0^1 \tilde{T} d\zeta} = 1 \tag{26}$$

and the constant molar density model yields the same results of the variable density one, while the results from the constant mass density model still yields different values.

The ratio between the evaporation rate predictions from the constant mass and molar density models can be expressed as follows:

$$M = \frac{Y^{mass}}{Y^{mol}} = \frac{1}{1+\theta\left(1-\chi_{ref}^{(1)}\right)} \frac{\ln\left(\frac{1-\chi_\infty^{(1)}}{1-\chi_s^{(1)}}\right)}{\ln\left(\frac{1-y_\infty^{(1)}}{1-y_s^{(1)}}\right)} \tag{27}$$

revealing that this ratio is only a function of the drop temperature and composition and the total pressure $M = M\left(T_s, Mm^{(1)}, P_T\right)$.

To better appreciate the model performances in some applicative conditions, three liquids are selected to represent different applications: water (fire control), n-octane (gasoline engines) and n-dodecane (aeronautic or Diesel engines) [10,11]. All the results presented in the following paragraphs are obtained setting $y_\infty^{(1)} = 0$.

Figure 1 shows the values of the $M = \frac{Y^{mass}}{Y^{mol}}$, equation (27), for the three selected liquids, as function of the drop temperature, which has been varied from 280K up to the boiling temperature at the selected total pressure, and for different values of total pressures representative of each liquid applicative conditions. The selected pressures were chosen to cover a range of applicative conditions bounded from above by the critical pressure for each species. The boiling temperatures, corresponding to each total pressure, are also reported. The results show that the differences between the constant mass and molar evaporation models are within few percentages (less than 4%) for water drops (Figure 1a) and they reduce decreasing the drop temperature. The constant mass density model underpredicts (relatively to the constant molar density model) the evaporation rate as the drop temperature increases, but when the drop approaches the boiling values the opposite behaviour is shown. Equation (27) reveals that, for each back pressure and liquid, a drop temperature closer to the boiling value can be found where the two models predict identical results ($M$=1). The test cases with n-octane (Figure 1b) and n-dodecane (Figure 1c) show larger discrepancies between the two constant density models, in particular when the drop temperature approaches the boiling temperature.

The values of the non-dimensional evaporation rate predicted by the three proposed models (see equations 11) are shown in Figure 2 for a water drop evaporating under atmospheric pressure conditions and gas temperature fixed equal to 1000K, with the drop temperature varying from 280K up to the boiling value. The results for this particular case show that both the constant density models overpredict the evaporation rate. To better appreciate the differences among the three models, Figure 3 shows the ratio between the values predicted by the two constant density models (molar and mass) and the values predicted by the variable density model (assumed as reference case) for water drop evaporating under atmospheric pressure conditions and three gas temperatures equal to 500, 1000 and 1500K. The drop temperature has been changed within the same range of Figure 2.

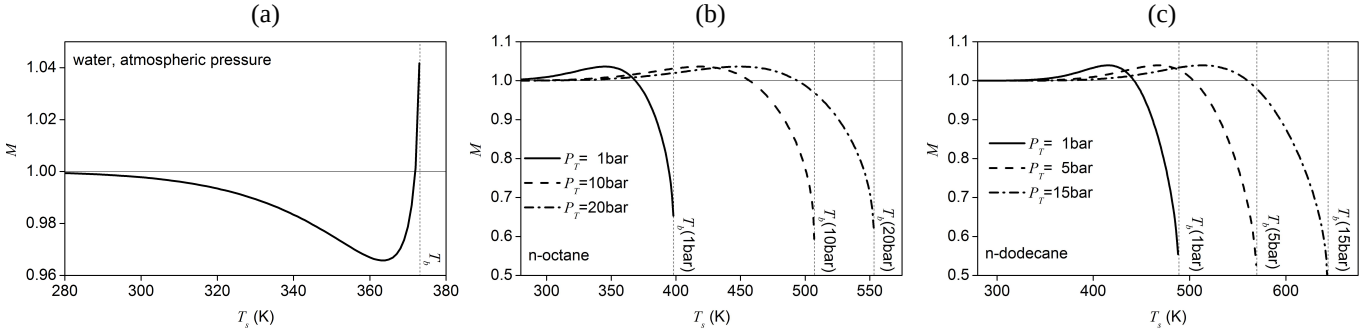


**Figure 1** Mass/molar evaporation rate ratio as function of drop temperature for (a) water drop at atmospheric pressure, (b) n-octane drop at 1, 10 and 20bar and (c) n-dodecane drop at 1, 5 and 15bar.

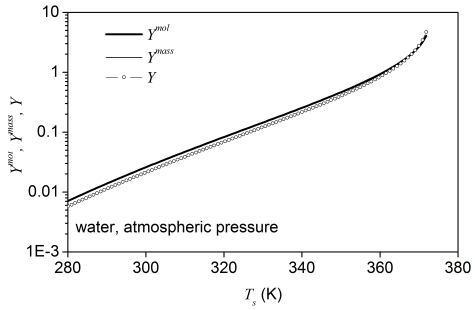


**Figure 2** Non-dimensional evaporation rate predicted by the three models as function of drop temperature for water drop at atmospheric pressure.

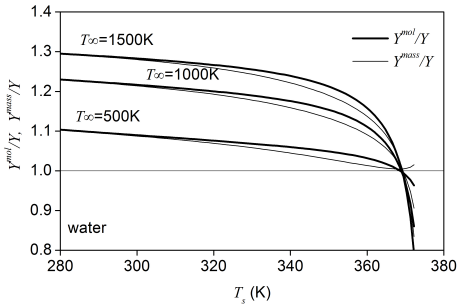


**Figure 3** Non-dimensional evaporation rate ratio as function of drop temperature at three gas temperatures for water drop at atmospheric pressure.

The results show that the two constant density models overpredict the evaporation rate (compared to the variable density one) except for a small range of drop temperature close to the boiling condition, and the overprediction increases with the gas temperature.

The same analysis was performed for the hydrocarbon liquids (n-octane and n-dodecane) and the results are reported in Figures 4 and 5, respectively, for the total pressures reported in Figure 1 (1, 10 and 20bar for n-octane and 1, 5 and 15bar for n-dodecane). At relatively low temperature, far from the liquid boiling point at the given pressure, both constant density models overpredict the evaporation rate, and the discrepancy increases with gas temperature. When drop temperature increases the evaporation rate predicted by both constant density models approaches the reference value, with the constant molar density model showing a closer agreement with the reference values.

Around a temperature not far from the liquid boiling temperature, the constant molar density model inverts the behaviour, underpredicting the reference value. The constant mass density model shows a similar behaviour, but the temperature at which the trend is inverted depends more on the gas temperature. As a general remark, for both hydrocarbons and all the selected back pressures, the constant molar density model yields evaporation rate prediction closer to the reference value for a larger drop temperature interval, while close to the drop boiling temperature both models tend to underpredict it and there exists only a small drop temperature interval where the constant mass density model behaves better.

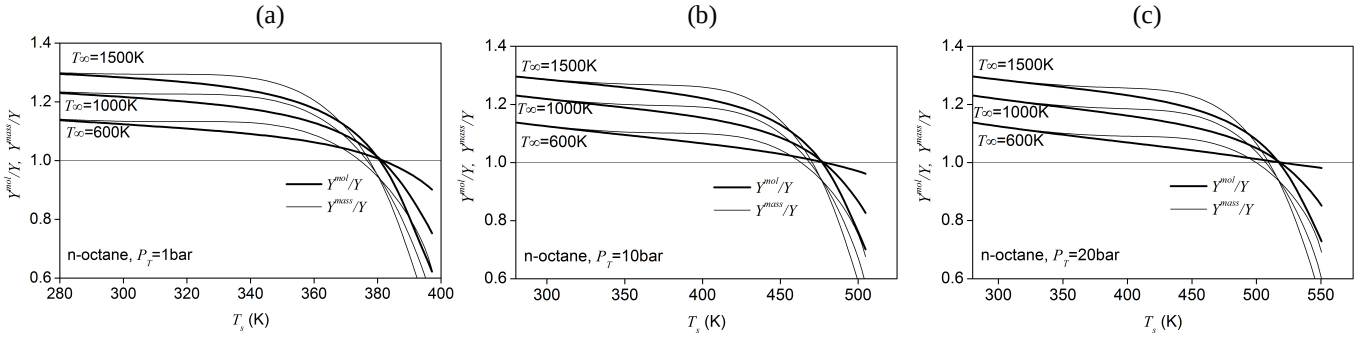


**Figure 4** Non-dimensional evaporation rate ratio as function of drop temperature at three gas temperatures for n-octane drop at (a) 1bar, (b) 10bar and (c) 20 bar.

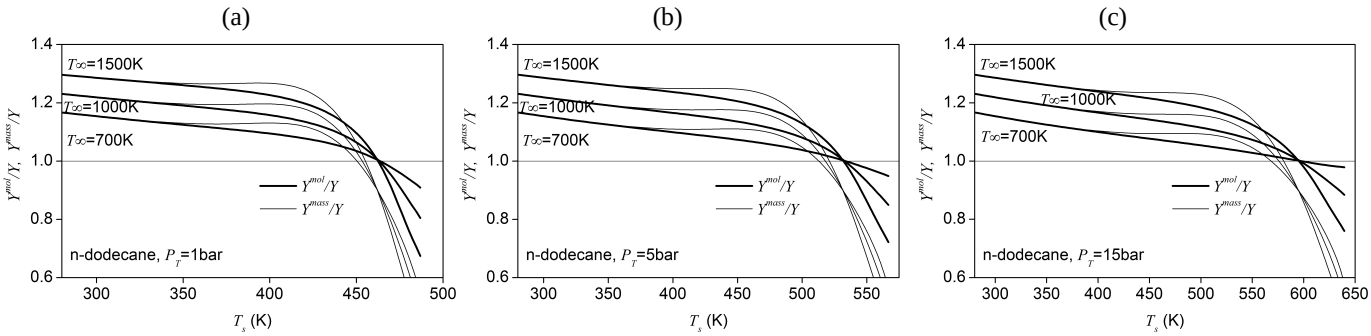


**Figure 5** Non-dimensional evaporation rate ratio as function of drop temperature at three gas temperatures for n-dodecane drop at (a) 1bar, (b) 5bar and (c) 15 bar.

## CONCLUSIONS

Two drop evaporation models based on the common assumption of constant gas density are compared to a novel model that relieves the cited assumption, and the following conclusion are summarised:

- the two constant density models predict similar values of the evaporation rate for drop temperature far from the boiling point, but the discrepancy increases when drop temperature approaches the boiling condition;
- both constant density models overpredict the evaporation rate when compared to the variable density model, which is taken as a reference in this study, for temperature far from the boiling temperature and by larger values as the gas temperature increases, showing that for evaporation in hot environment (combustion) these models may become less reliable;
- the constant molar density model appears to be more reliable than the constant mass density one for a large range of drop temperature at all the tested gas temperatures and pressures.

## REFERENCES

[1] S.S. Sazhin, Advanced models of fuel droplet heating and evaporation, *Prog. Energy Combust. Sci.*, Vol. 32, 2006, pp. 162-214.

[2] S. Sazhin, Droplet and sprays, Springer, 2014.

[3] Abramzon, B., Sirignano, W.A.: Droplet vaporization model for spray combustion calculations, *Int. Journal of Heat and Mass Transfer*, Vol. 32 (9), 1989, pp. 1605-1618.

[4] S. Tonini, G.E. Cossali, An analytical model of liquid drop evaporation in gaseous environment, *Int. Journal of Thermal Sciences*, Vol. 57, 2012, pp. 45-53.

[5] S. Tonini, G.E. Cossali, A novel vaporisation model for a single-component drop in high temperature air streams, *Int. Journal of thermal Sciences*. Vol. 75, 2014, pp. 194-203.

[6] J.C. Slattery, Momentum, Energy and Mass Transfer in Continua, second ed., Vol. 482, R. Krieger Publ., New York, 1981.

[7] S. Tonini, G.E. Cossali, A multi-component drop evaporation model based on analytical solution of Stefan-Maxwell equations, *Int. Journal of Heat and Mass Transfer*, Vol. 92, 2016, pp. 184-189

[8] N.A. Fuchs, Vaporisation and droplet growth in gaseous media, Pergamon Press, London, 1959.

[9] M.C. Yuen, L.W. Chen, On drag of evaporating droplets, *Combust. Sci. Tech*., Vol. 14, 1976, 147-154.

[10] D.R. Sobel, L.J. Spadaccini, Hydrocarbon Fuel Cooling Technologies for Advanced Propulsion, *ASME Journal of Engineering for Gas Turbines and Power*, Vol. 119, 1997, pp. 344-351.

[11] Z. Luo, S. Som, S.M. Sarathy, M. Plomer, W.J. Pitz, D.E. Longman, T. Lu, Development and validation of an n-dodecane skeletal mechanism for spray combustion applications, *Combustion theory and modelling*, Vol. 18(2), 2014, pp. 187-203.